

Electrically generated unidirectional surface plasmon source

L. Wang,¹ T. Li,^{1,*} L. Li,¹ W. Xia,² X. G. Xu,² and S. N. Zhu¹

¹National Laboratory of Solid State Microstructures, School of Physics, College of Engineering and Applied Sciences, Nanjing University, Nanjing 210093, China

²State Key Laboratory of Crystal Materials, Shandong University, Jinan 250100, China
taoli@nju.edu.cn

Abstract: We experimentally demonstrated an electrically excited surface plasmon source, which was fulfilled in a silver coated light emitting diode (LED) with well designed gratings. With a DC current supply, surface plasmon polariton (SPP) waves were generated directly from the illuminations of the LED via the grating coupler. By adjusting the grating to a tilted one, a unidirectional SPP beam was successfully attained with a high extinction ratio ($E_R \sim 10$) and an improved launching efficiency. Detailed analyses show that this electrically generated unidirectional SPP has a considerable long propagation distance ($\sim 14 \mu\text{m}$), allowing for further manipulations in plasmonic integrations and sensors.

©2012 Optical Society of America

OCIS codes: (240.6680) Surface plasmons; (230.2090) Electro-optical devices; (230.3670) Light-emitting diodes; (250.5403) Plasmonics.

References and links

1. E. Ozbay, "Plasmonics: merging photonics and electronics at nanoscale dimensions," *Science* **311**(5758), 189–193 (2006).
2. T. W. Ebbesen, H. J. Lezec, H. F. Ghaemi, T. Thio, and P. A. Wolff, "Extraordinary optical transmission through sub-wavelength hole arrays," *Nature* **391**(6668), 667–669 (1998).
3. K. Okamoto, I. Niki, A. Shvartser, Y. Narukawa, T. Mukai, and A. Scherer, "Surface-plasmon-enhanced light emitters based on InGaN quantum wells," *Nat. Mater.* **3**(9), 601–605 (2004).
4. Z. C. Dong, X. L. Zhang, H. Y. Gao, Y. Luo, C. Zhang, L. G. Chen, R. Zhang, X. Tao, Y. Zhang, J. L. Yang, and J. G. Hou, "Generation of molecular hot electroluminescence by resonant nanocavity plasmons," *Nat. Photonics* **4**(1), 50–54 (2010).
5. W. Cai, A. P. Vasudev, and M. L. Brongersma, "Electrically controlled nonlinear generation of light with plasmonics," *Science* **333**(6050), 1720–1723 (2011).
6. S. I. Bozhevolnyi, V. S. Volkov, E. Devaux, J. Y. Laluet, and T. W. Ebbesen, "Channel plasmon subwavelength waveguide components including interferometers and ring resonators," *Nature* **440**(7083), 508–511 (2006).
7. D. K. Gramotnev and S. I. Bozhevolnyi, "Plasmonics beyond the diffraction limit," *Nat. Photonics* **4**(2), 83–91 (2010).
8. J. A. Schuller, E. S. Barnard, W. Cai, Y. C. Jun, J. S. White, and M. L. Brongersma, "Plasmonics for extreme light concentration and manipulation," *Nat. Mater.* **9**(3), 193–204 (2010).
9. A. J. Haes and R. P. Van Duyne, "A unified view of propagating and localized surface plasmon resonance biosensors," *Anal. Bioanal. Chem.* **379**(7-8), 920–930 (2004).
10. K. A. Willets and R. P. Van Duyne, "Localized surface plasmon resonance spectroscopy and sensing," *Annu. Rev. Phys. Chem.* **58**(1), 267–297 (2007).
11. S. Lal, S. Link, and N. J. Halas, "Nano-optics from sensing to waveguiding," *Nat. Photonics* **1**(11), 641–648 (2007).
12. L. Yin, V. K. Vlasov, J. Pearson, J. M. Hiller, J. Hua, U. Welp, D. E. Brown, and C. W. Kimball, "Subwavelength focusing and guiding of surface plasmons," *Nano Lett.* **5**(7), 1399–1402 (2005).
13. Z. W. Liu, J. M. Steele, W. Srituravanich, Y. Pikus, C. Sun, and X. Zhang, "Focusing surface plasmons with a plasmonic lens," *Nano Lett.* **5**(9), 1726–1729 (2005).
14. A. Drezet, D. Koller, A. Hohenau, A. Leitner, F. R. Aussenegg, and J. R. Krenn, "Plasmonic crystal demultiplexer and multiplexers," *Nano Lett.* **7**(6), 1697–1700 (2007).
15. L. Li, T. Li, S. M. Wang, C. Zhang, and S. N. Zhu, "Plasmonic Airy beam generated by in-plane diffraction," *Phys. Rev. Lett.* **107**(12), 126804 (2011).
16. L. Li, T. Li, S. M. Wang, S. N. Zhu, and X. Zhang, "Broad band focusing and demultiplexing of in-plane propagating surface plasmons," *Nano Lett.* **11**(10), 4357–4361 (2011).
17. D. M. Koller, A. Hohenau, H. Ditlbacher, N. Galler, F. Reil, F. R. Aussenegg, A. Leitner, E. J. W. List, and J. R. Krenn, "Organic plasmon-emitting diode," *Nat. Photonics* **2**(11), 684–687 (2008).

18. R. J. Walters, R. V. A. van Loon, I. Brunets, J. Schmitz, and A. Polman, "A silicon-based electrical source of surface plasmon polaritons," *Nat. Mater.* **9**(1), 21–25 (2010).
19. P. Neutens, L. Lagae, G. Borghs, and P. Van Dorpe, "Electrical excitation of confined surface plasmon polaritons in metallic slot waveguides," *Nano Lett.* **10**(4), 1429–1432 (2010).
20. F. López-Tejiera, S. G. Rodrigo, L. Martín-Moreno, F. J. García-Vidal, E. Devaux, T. W. Ebbesen, J. R. Krenn, I. P. Radko, S. I. Bozhevolnyi, M. U. González, J. C. Weeber, and A. Dereux, "Efficient unidirectional nanoslit couplers for surface plasmons," *Nat. Phys.* **3**(5), 324–328 (2007).
21. J. J. Chen, Z. Li, S. Yue, and Q. H. Gong, "Efficient unidirectional generation of surface plasmon polaritons with asymmetric single-nanoslit," *Appl. Phys. Lett.* **97**(4), 041113 (2010).
22. J. J. Chen, Z. Li, S. Yue, and Q. H. Gong, "Highly efficient all-optical control of surface-plasmon-polariton generation based on a compact asymmetric single slit," *Nano Lett.* **11**(7), 2933–2937 (2011).
23. A. Baron, E. Devaux, J. C. Rodier, J. P. Hugonin, E. Rousseau, C. Genet, T. W. Ebbesen, and P. Lalanne, "Compact antenna for efficient and unidirectional launching and decoupling of surface plasmons," *Nano Lett.* **11**(10), 4207–4212 (2011).
24. These 400 dipole sources are linearly placed with an interval of $dL = 50$ nm (much than the grating period) and oriented along x -direction for the purpose of efficient TM excitation. In simulations, we calculated the illumination process of these 400 dipoles in total for one time with well-defined dipole locations, phases and polarizations. Although it is a coherent process, it can provide preliminary information of the coupling from the dispersive LED illumination to the SPP surface waves.

1. Introduction

Plasmonics, considered as a bridge between micro-scale photonics and nano-scale electronics [1], has boosted numerous researches in enhanced light-matter interactions [2–5], compact photonic circuits [6–8], biochemical events [9,10]. Versatile devices based on surface plasmon polaritons (SPPs) have been proposed and experimentally demonstrated in routing the energy in micro/nano scales [11–16]. Conventionally, light can be coupled into SPPs via coupling processes (e.g., using a prism or grating) to match the momentums of photon and surface plasmon, but these methods usually require a carefully adjusted external laser, which is bulky and inconvenient for compact integrations. Recently, several approaches have been developed by combining plasmonic system to the conventional electro-optical devices, in which SPP can be electrically generated without any external illuminations, for examples, in organic LEDs [17], silicon nanocrystals [18], and quantum-well LEDs [19]. These works enlightened the avenue that links the plasmonics to nowadays electronic world, whereas problems still remain open and need to be solved before achieving the practical active integrations. For instance, propagation length of these electrically generated SPP is severely limited (several micros [18,19]) and the generation efficiency was not evaluated, which are both of great importance in practical SPP integrations. Actually, to generate high efficiency and unidirectional plasmon wave has turned to be a major goal in the study of the plasmonics in recent years. Many efforts have been made based on various strategies of launching SPP from external lasers [20–23]. Therefore, electrically pumped SPP source with improved efficiency and unidirectional property would be an important step towards the compact active integration of SPPs.

In this work, we experimentally demonstrated an integrated SPP source based on micro-scale silver grating structures on a GaAs-based LED substrate that can be electrically excited. This generated SPP exhibits relative long propagation distance at the wavelength of $\lambda_0 \sim 633$ nm (GaAs-base LED). More importantly, this design was further developed to a unidirectional SPP generator by introducing tilted metallic gratings, and a high extinction ratio of $E_R \sim 10$ was experimentally achieved. This electrically generated SPP source is expected to be compatible with those passive devices in SPP manipulations, and would pave the way towards to active-plasmonic integrations.

2. Model and sample fabrication

The design of electrical excited SPP source is schematically shown in Fig. 1(a), in which an optically thick silver film (~ 200 nm) with gratings covers on the GaAs-based LED (detailed layer design and thickness are indicated in the figure). In the scheme, the illumination from the actively layer (Multi-Quantum-Well MQW) incidents onto the grating (defined as source grating), and then transfers to two bidirectional surface SPP waves by the coupling processes.

Since the surface waves cannot be directly observed in the far field, two sets of groove gratings are introduced as out-couplers symmetrically on both sides of coupling grating with certain distances. As indicated in the scheme, two out-couplers will scatter the propagating SPP waves into the far field that can be detected by charge-coupled device (CCD), despite there will be still considerable illumination transmitted directly through the center source grating. These scattered intensities (from the out-couplers) will be referred for evaluating the efficiency of the generated SPP wave qualitatively.

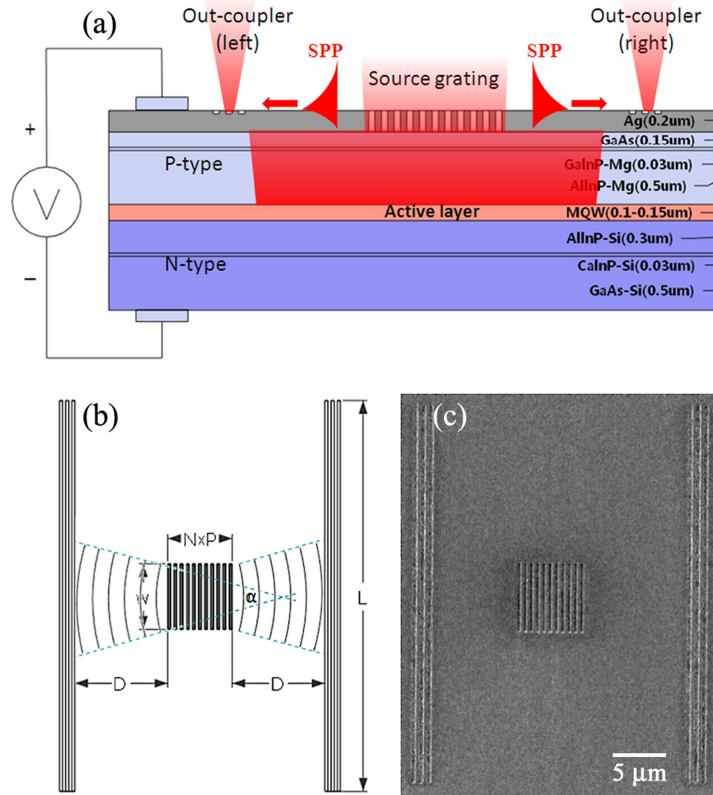


Fig. 1. (a) Schematics of electrically excited SPP source with the combination of GaAs-based LED and silver film with structured coupling grating and out-coupler grooves, where detailed LED structural parameters are marked on. (b) Designed planar structures for experiments. (c) FIB image of the fabricated sample corresponding to the design, where $N=11$, $P=0.61 \mu\text{m}$, $D=10 \mu\text{m}$, $W=6.4 \mu\text{m}$, $L=35 \mu\text{m}$.

The samples are fabricated by the focused ion beam (Strata FIB 201, FEI Company, 30 KeV, 11 pA) milling on a sputtered silver film ($\sim 200 \text{ nm}$ thickness). Figure 1(b) and 1(c) are the top view of the source grating and out-couplers for schematic design and real sample, respectively. Here, the source grating is composed of 11 slits with period of 610 nm (corresponding to the $\lambda_0 \sim 633 \text{ nm}$ of the LED illumination) and slit length of $6.4 \mu\text{m}$ and width of 300 nm . Therefore, the footprint of device is about $6.4 \times 6.4 \mu\text{m}^2$. The shallow grooves for out-coupling are $35 \mu\text{m}$ long and only 30 nm depth (in order to forbid the direct transmission of the underneath illuminations). Much longer grooves than the coupling grating is designed to analyze the beam shape of the SPPs via comparison from the far field radiation signals.

3. Numerical simulations and experimental results

Before getting into the experimental details, we would rather firstly show the theoretical results calculated using commercial software (Lumerical FDTD solutions). In the model, 400 dipoles as a 2-dimensional (2D) random source are defined to mimic the MQW active layer [24], which is set 0.68 μm distance from the metal layer as shown in Fig. 1(a) (according to the experimental sample parameters). The dielectric constant of metal and semiconductor are designed as $\varepsilon_{\text{Ag}} = -15.932 + 1.076i$ and $\varepsilon_{\text{GaAs}} = 14.826 + 1.507i$ (at $\lambda_0 = 633 \text{ nm}$, in the database of Lumerical solver). The structural parameters are defined as possible as experimentally reachable ($P = 610 \text{ nm}$, $D = 10 \mu\text{m}$).

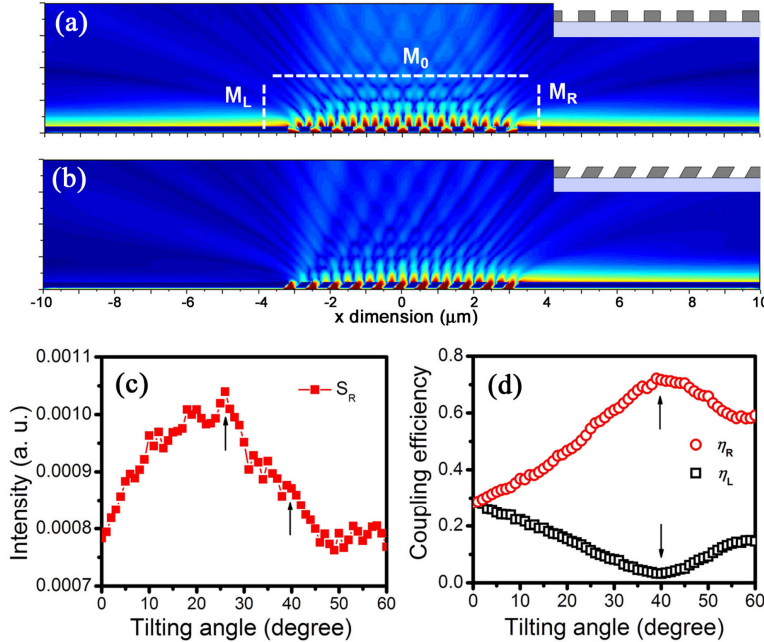


Fig. 2. Simulation results of the SPP field generation by the source grating for (a) normal grating and (b) 40°-tilted grating under a defined chaotic source (containing 400 random dipoles) in the active layer mimicking the LED. Dashed lines in (a) are introduced monitors to detect the energy flow around the sources gratings. (c) Power intensity detected by right monitor (M_R) as the function of tilting angle of the source grating. (d) Normalized coupling coefficient of the right and left propagating SPPs (defined as η_R and η_L) with increasing the tilting angle, where a maximum contrast is mark out at $\theta = 40^\circ$.

Figure 2(a) depicts the simulated field distribution (H_y), from which two obvious bidirectional surface waves are generated by the grating coupling from the illumination of random dipoles in the active layer, where considerable amount of energy still radiate to the far field directly through the grating. It is undoubted that these surface waves are the SPPs by checking their polarizations (little E_y detected for the surface waves). Three monitors are place on the top (M_0), left (M_R) and right (M_L) of the source grating (shown in the figure), to detect the corresponding energy flows. Calculating the ratio of $\eta_R = S_R / (S_0 + S_R + S_L)$ and $\eta_L = S_L / (S_0 + S_R + S_L)$ ($S_{i(i=0,R,L)}$ refers to the energy flow from the monitor M_i), we would roughly evaluate the coupling efficiencies from the illumination to the SPPs. Although it is somewhat rough by neglecting the absorption and reflection of the grating, it is still of importance to evaluate the performance of the SPP source. Since the direct radiation of S_0 always brings noises for a plasmonic device, the higher ratio η indicates the better coupling, and the better

quality of the SPP source. For the case of the normal grating shown in the inset image of Fig. 2(a), the SPP coupling processes are symmetric and $\eta_R = \eta_L \approx 0.24$. When we modified the source grating to be tilted with an angle of θ , the symmetry will be broken and the right side coupling tends to be enhanced, as shown in Fig. 2(b). Figure 2(c) depicts the detected power intensity of S_R as a function of the tilting angle, which exhibits a clear increase with the enlarged angle and reaches a maximum at about $\theta = 26^\circ$. By analyzing the tendencies of coupling ratio η_R and η_L (shown in Fig. 2(d)), we find they departure expectedly with respect to the increasing θ and have a strongest contrast at $\theta = 40^\circ$, where η_L tends to be zero. These calculations provide us a fascinating result that we can adjust the tilting angle to achieve a unidirectional generation of SPP. Although the power flow of S_R of $\theta = 40^\circ$ is not the highest one (refer to Fig. 2(c)), the largest coupling efficiency η_R and highest extinction ratio ($E_R = \eta_R / \eta_L \approx 24$) implies that this sample should have the best unidirectional performance. Therefore, this sample will be particularly studied in comparison with the normal grating sample in experiments.

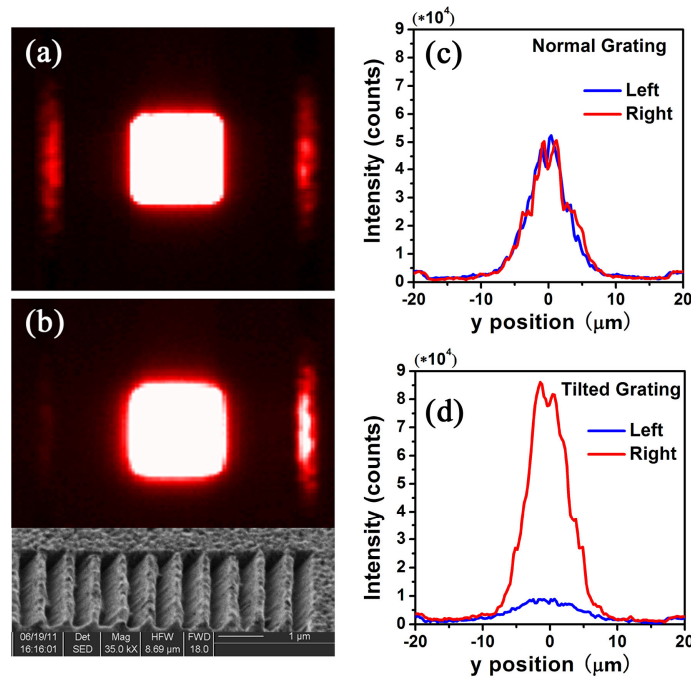


Fig. 3. Microscope imaged scattered intensities from source grating and out-coupler grooves under a DC current excitation ($\sim 100 \text{ mA/cm}^2$) for the (a) normal grating sample and (b) 40° -tilted grating one. The FIB image of tilted sample is shown in the bottom of (b). (c) and (d) are the extracted intensity data of two out-couplers from the images (a) and (b) respectively, where a strong contrast of right and left scattered SPPs are clearly observed in the titled grating sample.

Two samples with the same planar parameters ($N=11$, $P=0.61 \mu\text{m}$, $D=10 \mu\text{m}$, $W=6.4 \mu\text{m}$, $L=35 \mu\text{m}$) but different source gratings were particularly analyzed: sample A for normal grating $\theta \sim 0^\circ$ (the designed and FIB images are shown in Fig. 1(b) and 1(c), respectively) and sample B for $\theta \sim 40^\circ$ (see the oblique image in bottom of Fig. 3(b)). Optical analyses were performed in a microscopy system (Zeiss AxioImager-A1m) with EM-CCD camera (Andor DU888) by adopting a bias DC current about 100 mA/cm^2 (corresponding to $\sim 2.4 \text{ V}$ voltage for our samples). Figure 3(a) shows the experimental image directly recorded by the CCD, where an obvious scattered SPP after propagation a certain distance ($10 \mu\text{m}$) are observed for sample A. This SPP generation is expectedly bidirectional due to the symmetric coupling

process, which is also reflected from the well superposed intensity profiles read from the out-coupling intensity curves (see Fig. 3(c)). The SPP nature was further confirmed by the fact that little out-coupling intensity was detected by adding a polarizer to check the TE case (polarization along the out-coupler groove direction) (not shown here). As for the sample B with the tilted grating ($\theta=40^\circ$), apparent unidirectional SPP generation is shown in Fig. 3(b), where most of SPP energy flows to the right and a considerably large extinction ratio $E_R \sim 10$ is achieved from the data of Fig. 3(d). Although this value is smaller than those launched by lasers [21, 23], it is still a good performance in the electrically excited LED system. Moreover, the absolute intensity of the right-propagation SPP increases to 1.7 times the bidirectional ones in Fig. 3(b). It is definitely proved that using metallic grating can remarkably couple the dispersive LED illumination into a unidirectional SPP wave with improved coupling efficiency.

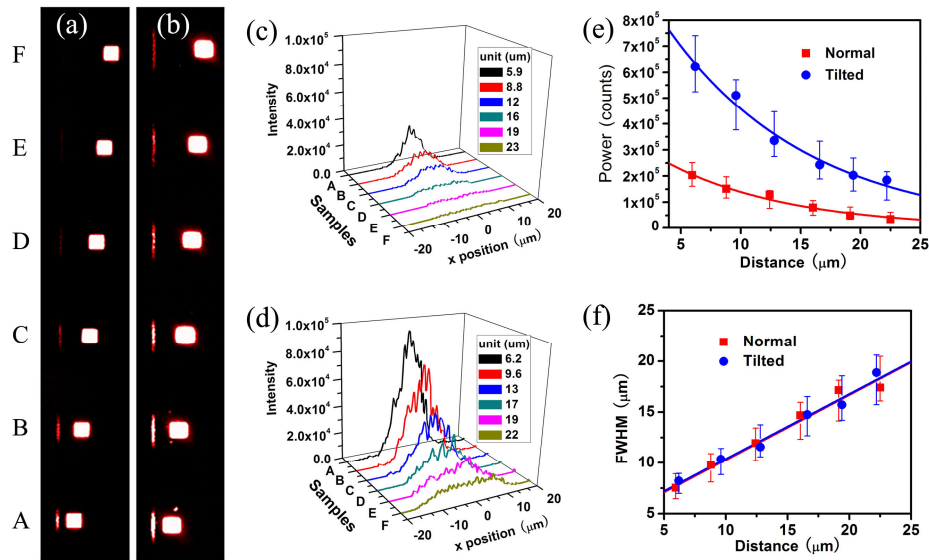


Fig. 4. Direct microscope images of samples for the (a) normal grating series and (b) tilted grating series with different groove-to-grating distances, which are indicated by capitals “A-F”. Detailed intensity profiles of the scattered SPPs at out-coupler for series samples: (c) normal grating sample, (d) tilted grating sample. (e) Integrated power intensity of experimental data as versus different propagation distances for two series sample, where curves are the exponentially fitted ones. (f) The detected FWHMs as the function of propagation distances for both samples.

In the following, two series of samples are fabricated with different out-coupling distance (D) both for normal and titled gratings in order to make detailed analyses on the generated SPP beam properties. Using a stabilized power supply as same as the former experiment (DC current $\sim 100 \text{ mA/cm}^2$), the emission power and spectrum of the LED was kept constant to establish a standard backlight illumination. The CCD detected intensities from the out-couplers are in proportion to the SPP intensities at the detection positions, which provide us a quantitative evaluation on the generated SPP wave. Figure 4(a) and 4(b) show the direct CCD images of the normal and tilted grating samples respectively with D ranging from about 5 to 23 μm (labeled by capitals A to F in the left margin), where different intensity evolutions with respect to the SPP propagation distances are clearly manifested. The detailed intensity profiles at different distances are further depicted out in the Fig. 4(c) and 4(d) for these two series samples. The coupling improvement of titled sample is shown obviously. By analyzing these intensity profiles we can obtained the detailed information of the evolution of the field distributions, so as to deduce the propagation property of the generated SPP waves. Figure 4(e) shows the detected power evolutions of two SPP propagations, where remarkable

enhancement (more than 3 times) of the titled sample are definitely demonstrated at the initial position, indicating a greatly improved coupling efficiency. By exponential fitting on the experimental data, we obtained the decay lengths of both cases of about $11.0 \mu\text{m}$ and $13.7 \mu\text{m}$, respectively. The tilted sample still manifests a little advantage in propagation distance. So far, a well defined unidirectional SPP source with electrical excitation is achieved.

4. Discussions

We would briefly explain the cause of unidirectional coupling process by titled grating in the viewpoint of reciprocal vectors. We made a Fourier transformation (FT) on the titled grating structure, and then the real space information can be converted to the reciprocal space. Figure 5(a) shows FT result directly from the x - z cut plane of the grating (inset image on the left bottom), where the reciprocal lattice with the strongest Fourier components inclines with the same angle as the titled grating, resulting in two strongest first-order reciprocal vectors in -40° angle for the right one ($G_{1,0}$) and 40° angle for the left one ($G_{-1,0}$). In LED illuminations, although the radiation is dispersive, the majority is still normal to the grating plane. As schemed in Fig. 5(b), these normally radiated lights will be more easily coupled to the right side after the vector combination, resulting in a right propagation SPP wave.

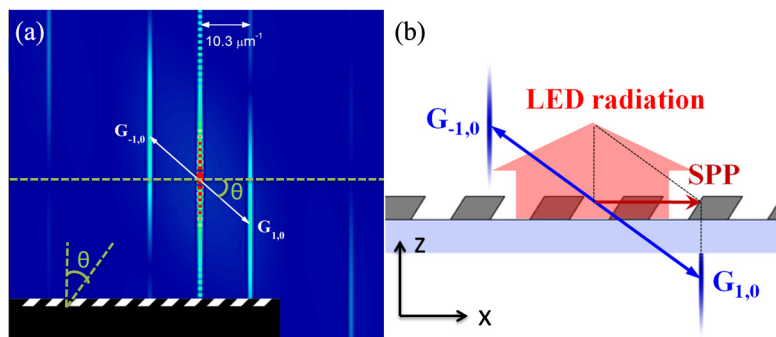


Fig. 5. (a) Reciprocal space of the 40° -tilted grating, where the inset image is real space cross-section of the grating in x - z cut plane. (b) Scheme of the wave vector combinations explaining the unidirectional SPP generation.

Besides, the full widths at half-maximum (FWHM) of the two generated SPP waves are also depicted in Fig. 4(f), who have almost the same fitting lines. It means that the generated SPP waves from two samples still maintain the same propagation characteristics, though they have different coupling efficiency. This increasing FWHM indicates the electrically generated SPP beam is dispersive. By evaluating FWHM tendency, we find that this kind of SPP wave exhibits a considerable large spreading angle ($\alpha \sim 30^\circ$) compared with the conventional SPP Gaussian beam excited by laser. This is due to the nondirectional LED illumination, which has loose dependence on the grating parameter for its complex k vectors. Nevertheless, a considerable strong SPP wave with unidirectional beaming was definitely generated by electrical pumping on the basis of GaAs-based LED without any additional light source. A high normalized coupling efficiency (about 70%, theoretical) was predicted in the titled grating sample, and a relative long propagation distance ($\sim 14 \mu\text{m}$) was experimentally obtained allowing for further manipulation of this generated SPP wave.

5. Conclusions

In summary, we experimentally demonstrated a LED-based SPP source with an almost unidirectional beaming property, which was directly excited by a DC current in a very convenient manner. Base on a tilted grating design, this achieved unidirectional SPP exhibited a considerable large extinction ratio ($E_R \sim 10$) and long propagation distance ($\sim 14 \mu\text{m}$), which is a remarkably good performance considering the illumination is not from a coherent laser

but the chaotic and nondirectional LED. This device is only about $6.4 \times 6.4 \mu\text{m}^2$ footprint (for the source grating part) indicating a compact active integration is achievable. Our experiment would inspire versatile applications in plasmonic circuitry or bio-sensors, and is expected to step the way toward bridging the gap between electronic and photonic devices.

Acknowledgments

This work is supported by the State Key Program for Basic Research of China (Nos. 2009CB930501, 2012CB921501, 2010CB630703 and 2011CBA00200), the National Natural Science Foundation of China (Nos. 10974090, 11174136, 11021403 and 60990320) and PAPD of Jiangsu Higher Education Institutions.